Manuscript prepared for Atmos. Chem. Phys.
with version 5.0 of the LaTeX class copernicus.cls.
Date: 10 November 2014

A global process-based study of marine CCN trends and variability

E. M. Dunne[1], S. Mikkonen[2], H. Kokkola[1], and H. Korhonen[3]

[1]Finnish Meteorological Institute, Atmospheric Research Centre of Eastern Finland, P.O. Box 1627, 70211 Kuopio, Finland
[2]University of Eastern Finland, Department of Applied Physics, P.O. Box 1627, 70211 Kuopio, Finland
[3]Finnish Meteorological Institute, Climate Research, P.O. Box 503, 00101 Helsinki, Finland

Correspondence to: E. M. Dunne (eimear.dunne@fmi.fi)

Abstract. Low-level clouds have a strong climate-cooling effect in oceanic regions due to the much lower albedo of the underlying sea surface. Marine clouds typically have low droplet concentrations, making their radiative properties susceptible to changes in cloud condensation nucleus (CCN) concentrations. Here, we use the global aerosol model GLOMAP to investigate the processes that determine variations in marine CCN concentrations, and focus especially on the effects of previously identified wind speed trends in recent decades. Although earlier studies have found a link between linear wind speed trends and CCN concentration, we find that the effects of wind speed trends identified using a dynamic linear model in the Northern Equatorial Pacific ($0.56\,\mathrm{ms}^{-1}$ per decade in the period 1990–2004) and the North Atlantic ($-0.21\,\mathrm{ms}^{-1}$ per decade) are largely dampened by other processes controlling the CCN concentration, namely nucleation scavenging and transport of continental pollution. A CCN signal from wind speed change is seen only in the most pristine of the studied regions, i.e. over the Southern Ocean, where we simulate $3.4\,\mathrm{cm}^{-3}$ and $0.17\,\mathrm{ms}^{-1}$ increases over the fifteen-year period in the statistical mean levels of CCN and wind speed, respectively. Our results suggest that future changes in wind-speed-driven aerosol emissions from the oceans can probably have a climate feedback via clouds only in the most pristine regions. On the other hand, a feedback mechanism via changing precipitation patterns and intensities could take place over most oceanic regions, as we have shown that nucleation scavenging has by far the largest absolute effect on CCN concentrations.

1 Introduction

Atmospheric aerosols are an important component in the Earth's climate system due to their ability to absorb and scatter solar and terrestrial radiation (Boucher et al., 2013). Overall, the largest source of aerosols are the oceans (Textor et al., 2006), which cover mor than 70 % of the Earth's surface area. The main aerosol types originating from the oceans are primary sea spray particles, which consist mainly of sea salt and organic matter (O'Dowd et al., 2004; Sciare et al., 2009; Gantt and Meskhidze, 2013), and DMS (dimethyl sulfide)-derived sulphate particles, which are formed via new particle formation from DMS oxidation products (Clarke, 1993; Bates et al., 1998). Previous research has highlighted the central role of both sea spray and sulphate particles in forming marine cloud condensation nuclei (CCN) (Clarke et al., 2006; Vallina et al., 2006; Pierce and Adams, 2006; Korhonen et al., 2008; Partanen et al., 2014). Since marine clouds typically contain relatively low cloud droplet concentrations (Quaas et al., 2006; Zheng et al., 2011), their albedos are susceptible to variations in oceanic CCN (Twomey, 1991).

The emission rates of both sea spray and DMS are strongly dependent on wind speed, with observations suggesting dependencies ranging from $\sim u_{10}^{2.3}$ to $\sim u_{10}^{3.4}$ for sea spray (Monahan and Muircheartaigh, 1980; Ovadnevaite et al., 2012) and $\sim u_{10}^{2}$ for DMS (Wanninkhof, 1992; Nightingale et al., 2000), where u_{10} is the 10-m wind speed. Such strong dependencies imply that long-term changes in oceanic surface wind speeds, e.g. as a result of climate change (Bracegirdle et al., 2013), could lead to substantial changes in marine aerosol emissions and CCN concentrations. Recently, Korhonen et al. (2010) used a global aerosol model to estimate that the observed intensification of the westerly jets in the Southern Ocean troposphere since the 1980s may have led to an increase of more than 20 % in CCN concentrations in the latitude band 50–65° S.

Significant surface wind speed changes have also been observed in other marine regions over the past three decades, but their effects on natural aerosol production have not been thus far investigated. Young et al. (2011) used satellite altimeter measurements over the years 1991–2008 to conclude that the mean wind speeds have increased by between 0.25 and 0.5 % per year over the majority of the world's oceans, with stronger trends in the Southern than in the Northern Hemisphere. On the other hand, Vautard et al. (2010) concentrated on the Northern Hemisphere and found a strong increasing wind trend in the Northern Equatorial Pacific evident in both NCEP/NCAR (1979–2008) (Kalnay et al., 1996) and ERA-Interim (1989–2008) (Dee et al., 2011) reanalyses. The ERA-Interim reanalysis also indicated smaller decreasing trends in the North Atlantic between latitudes 50° and 60° N, in the Caribbean Sea, and in the north-western Pacific.

Here we investigate the effect of past wind speed trends between the years 1990 and 2004 on the marine aerosol population by forcing an offline global aerosol model with meteorology from ERA-Interim reanalyses. The model accounts for the complex interplay between aerosol sources and sinks, and therefore allows us to quantify the relative roles of different atmospheric processes in determining the marine CCN concentrations. We also estimate how significant other processes, such

as new particle formation or wet scavenging, are compared to wind-related processes like sea spray or DMS emissions.

2 Methodology

2.1 GLOMAP

The global aerosol model GLOMAP-mode (Mann et al., 2010) is an extension to the TOMCAT 3-D chemical transport model (Chipperfield, 2006). It was run with a T42 spectral resolution ($2.8^\circ \times 2.8^\circ$) and with 31 hybrid σ-pressure levels extending to $10\,\mathrm{hPa}$. Since GLOMAP is an offline model, large-scale atmospheric transport is specified from ERA-Interim reanalysis, produced by the European Centre for Medium-Range Weather Forecasts (ECMWF), at 6 h intervals (Dee et al., 2011).

GLOMAP-mode uses a two-moment modal scheme to describe the aerosol size and composition distribution with seven log-normal modes and with five chemical components (sea salt, sulphate, organic carbon, black carbon, and dust). Four of the seven modes are water-soluble and expand the diameter ranges 3–10 nm, 10–100 nm, 100 nm–1 μ m and $> 1\,\mu$ m, respectively. The remaining three modes can contain only insoluble material (black and organic carbon, dust) and they cover the diameter ranges 10–100 nm, 100 nm–1 μ m and $> 1\,\mu$ m, respectively. In this study, CCN refers to particles with dry diameter of at least $70\,\mathrm{nm}$, and all quoted values are from the model level with pressure $930\,\mathrm{hPa}$.

The microphysical processes in GLOMAP-mode include intra- and intermodal coagulation, condensational growth of all modes as well as ageing of insoluble modes to soluble due to uptake of sulphuric acid and secondary organic vapours; new particle formation via nucleation; oxidation of SO_2 to SO_4 in cloud droplets; and wet and dry deposition. In this study, new particle formation is simulated using the parametrisation of Vehkamäki et al. (2002) in the free troposphere, with the activation-based scheme of Sihto et al. (2006) in the boundary layer. Wet deposition occurs in frontal and convective precipitating clouds through nucleation scavenging (i.e. activation of CCN into cloud droplets and subsequent removal by precipitation) and impaction scavenging (i.e. collection of particles by falling raindrops). The scavenging rates are calculated based on rain rates disagnosed from successive ECMWF analysis fields. Within the cloud, large-scale rain removes particles at a constant rate equivalent to 99.9 % conversion of cloud water to rain over $6\,\mathrm{h}$. For convective-scale rain, we use the Tiedtke (1989) convection parameterization to calculate the cloud-to-rain water converstion rate and assume a raining fraction of 0.3. The rainout is applied to soluble particles with dry diameter greater than $103\,\mathrm{nm}$. On the other hand, impaction scavenging is simulated using a look-up table for raindrop-aerosol collection efficiencies based on the Marshall–Palmer raindrop size distribution.

In this study, primary sea spray emissions are calculated according to the Mårtensson et al. (2003) parameterization, which also includes ultrafine emissions. Since the emitted sea spray modes ac-

cording to Mårtensson et al. (2003) are not strictly log-normal, we are not able to conserve both number and mass simultaneously when applying the parameterisation in GLOMAP-mode. The model conserves mass. Mineral dust emissions can be included via two wind-speed driven emissions parameterizations (Pringle, 2006; Manktelow et al., 2010) or as prescribed daily-varying fluxes described in Dentener et al. (2006). However, in this study, mineral dust was excluded. Oceanic DMS emissions are calculated based on the monthly sea-water DMS concentration climatology of Kettle and Andreae (2000) and the sea-air exchange parameterization of Nightingale et al. (2000). Continental SO_2 sources include anthropogenic emissions following Cofala et al. (2005), volcanic SO_2 emissions from Andres and Kasgnoc (1998) and Halmer et al. (2002), and monthly-varying biomass burning emissions following Van Der Werf et al. (2003). Primary carbonaceous aerosol emissions of black and organic carbon from fossil fuel and biofuel sources (Bond et al., 2004) and biomass burning (Van Der Werf et al., 2003) are taken into account. Secondary organic vapours are formed via gas-phase oxidation of monoterpene emissions following Guenther et al. (1995), and condense into the organic carbon component. Concentrations of oxidants are specified offline every six hours from a previous TOMCAT simulation (Arnold et al., 2005).

To detect any long-term CCN trends associated with recent wind speed changes, GLOMAP-mode was run for a 15 year period covering the years 1990–2004. From this long run, only monthly mean output was saved. Further insight into the processes determining marine CCN variability in different regions was gained by conducting additional two-month simulations with six-hourly output. In these shorter simulations, we switched off one process at a time in order to investigate its influence to the CCN concentration. The processes studied were: primary sea spray emissions, DMS emissions, new particle formation, impaction scavenging, and nucleation scavenging.

2.2 Statistical methods

The variability in the monthly-mean time series of 10-m wind speed (according to the ERA-Interim reanalysis) and the simulated CCN concentrations was investigated using a dynamic linear model (DLM) approach. Dynamic linear models are linear regression models where the regression coefficients can depend on time. This dynamic approach is well known and documented in time series literature (Chatfield, 2013; Harvey, 1990; Hamilton, 1994; Migon et al., 2005). The calculations were done with the R statistical language using the package dlm (Petris et al., 2009).

In this study, we were mainly interested in the long term trends in marine wind speed and CCN concentrations over the period of 1990–2004. Statistically speaking, a trend is a statistical change in the properties of the background state of the system (Chandler and Scott, 2011). Although changes in natural systems have previously been approximated with linear trends (e.g. wind speed in Vautard et al., 2010), this is not always the most appropriate approach, since such systems evolve continuously over time. Furthermore, time series of natural systems can include multiple time dependent cycles (e.g. seasonal and diurnal cycles) which are typically non-stationary – that is, their distribu-

tional properties change over time. The DLM approach can effectively decompose the time series into basic components, such as level, trend, seasonality and the effect of external forcing. All of these components can be allowed to change over time, and the magnitude of this change can be modelled and estimated. With a properly set-up and estimated DLM, the magnitude of the trend is not prescribed by the statistical model formulation and the method does not favour finding a "statistically significant" trend. The statistical model provides a method to detect and quantify trends, but it does not directly provide explanations for the observed changes, i.e., whether the changes in the background level could be explained by natural variability or some external shock. However, it can determine that the observations are consistent with the selected model.

We use DLM to explain variability in the wind and CCN time series using three components: smooth-varying locally linear mean level, seasonal effect, and noise that is allowed to have autoregressive correlation. The evolution of the investigated variables, after the seasonal and irregular noise components have been filtered out, is modelled using the mean level; here, the change in the mean level is the trend of the variable. If we denote the investigated variable (e.g. wind speed) at time t with y_t, we can write the statistical model as

$$y_t = \mu_t + \gamma_t + \eta_t + \epsilon_t, \quad t = 1, \ldots, N, \quad \text{with } \epsilon_t \sim N\left(0, \sigma_t^2\right) \tag{1}$$

where μ_t is the mean level at time t, γ_t is the seasonal component for monthly data, η_t is an autoregressive error component, and ϵ_t is the error term for the uncertainty in the observed values. All the model components are allowed to change with time and they are stochastic, defined by Gaussian distributions. The seasonal component γ_t contains dummy variables for each month, so γ_t has a different value for each month, with a condition that 12 consecutive months sum to zero, but, as the values are allowed to evolve in time, the condition holds only on the average.

3 Results and discussion

3.1 Changes in wind speeds and CCN concentrations during 1990–2004

First, we investigate whether the previously identified changes in marine wind speeds since the turn of the 1990s translate into trends in the simulated marine CCN concentrations. We concentrate on the period 1990–2004, and calculate the wind trends based on monthly mean gridded values from the ERA-Interim reanalysis, and the CCN trends based on monthly mean simulated values from GLOMAP.

Figure 1 presents the linear wind trend over the period of 1990–2004. The largest wind trend over the oceans has occurred in the Equatorial Pacific where the wind speed increase over much of this region has reached or even exceeded $0.5\,\mathrm{ms}^{-1}$ per decade. Locally, trends as high as $0.8\,\mathrm{ms}^{-1}$ per decade are evident. Parts of the Southern and Indian Oceans show increasing trends of around $0.3\,\mathrm{ms}^{-1}$ per decade. On the other hand, decreasing wind trends are evident in the Northern Atlantic

between 45° and 60° N, and in the Arctic over the Greenland and Barents seas. Both of these regions exhibit trends in the range of $-0.4\,\mathrm{ms}^{-1}$ per decade with local trends extending down to $-0.7\,\mathrm{ms}^{-1}$ per decade.

It should be remembered, however, that in reality the long-term change in wind speed is hardly ever strictly linear in the ERA-Interim data. Figure 2a compares different ways of looking at ten-metre winds in the Northern Equatorial Pacific region (indicated in Fig. 1, black box) for the period 1979–2012. The blue line plots raw data from the ERA-Interim re-analyses. The red line shows the mean wind level calculated using the DLM, while the green line shows the linear trend fit for the period 1990–2004. The linear trend in this region for 1990–2004 is $0.29\,\mathrm{ms}^{-1}$ per decade; however, upon closer inspection of the DLM it becomes clear that the mean wind level decreases between 1990 and 1993, increases between 1993 and 2000, and then decreases again between 2000 and 2004. It is evident that a linear fit is incapable of capturing the details of this behaviour. Furthermore, the calculated linear trend can be sensitive to the choice of analysis period, as illustrated in Fig. 2b for a North Atlantic region (shown with a black box in Fig. 1). The long-term mean wind level in this region shows a fairly smooth variation between wind speeds of 9.4 and $9.8\,\mathrm{ms}^{-1}$. However, a linear fit restricted to the 1990–2004 period gives start and end values of 10.1 and $9.4\,\mathrm{ms}^{-1}$, respectively, and clearly overestimates the change in the long-term mean wind level over this period. An example of a region where the linear approach works fairly well can be seen in the Southern Ocean (Fig. 1, black box), where the linear trend (Fig. 2c, green line) does not deviate from the locally linear mean level (red line). These shortcomings of the linear trend approach do not affect our CCN analysis since the GLOMAP model was forced with 6 hourly ERA-Interim meteorology and not with the calculated linear trends.

Similarly to the wind speed analysis in Fig. 2, we decomposed the simulated monthly-mean CCN time series over 1990–2004 to a smooth-varying mean level, a seasonal component and an irregular noise component (see Sect. 2.2). Figure 3 depicts the time evolution of the mean wind and CCN levels for the three marine regions shown in Fig. 1. These specific regions were chosen for closer analysis for the following reasons:

1. The Northern Equatorial Pacific region (0–20° N, 150–240° E) shows the strongest increasing linear trend of wind speed over the world's oceans (Fig. 1), but the mean wind level shows both increasing and decreasing behaviour during the studied period (Fig. 3a), making this region an interesting test case for finding a wind speed signal in the CCN concentration.

2. The North Atlantic region (50°–60° N, 310–340° E) shows a consistent decreasing trend in wind speed (Figs. 1 and 3c).

3. The Southern Ocean region (45–60° S, 45–80° E) shows an increasing trend (Figs. 1 and 3e) and is located in a remote area far away from continental pollution sources. Therefore, it can be expected that the main sources of CCN in this region are natural and therefore the effect of

wind speed trends on the CCN concentration should be easier to detect.

A comparison of the mean wind speed and CCN levels (Fig. 3 left and right panels, respectively) shows that there is no clear connection between the wind speed and CCN changes in the two northern hemispheric regions that have the strongest wind trends. In the Northern Equatorial Pacific region the overall mean levels of both wind speed and CCN increase over the study period; however, the time development of the two trends are very different (panels a and b). For example, much of the CCN increase takes place between 1990 and 1993 when the mean wind speed is decreasing. After that, the CCN concentration levels off between 1995 and 2000 while the wind speed shows a clear increasing trend. Similarly in the North Atlantic region, the CCN level shows a small increase until the year 2000 despite the decreasing wind trend (panels c and d). On the other hand, over the Southern Ocean, where CCN sources are expected to be predominantly oceanic, both wind speed and CCN show positive trends over the whole studied period (panels e and f). However, the shapes of the sea spray emission trend ($\sim u_{10}^{3.41}$, not shown) and the CCN trend are still quite different, with the CCN trend showing much steeper behaviour prior to year 2000 and then levelling off. We can see from Fig. 1 that the wind speed trends in the areas surrounding the patch of Southern Ocean being examined are quite different. Some of the differences between the trends in CCN and wind speed may be due to transport of aerosol from these other regions.

Interannual variations in sea-surface temperature are not accounted for in GLOMAP, as a climatology of sea-surface temperature is used and does not change from year to year. However, the Mårtensson et al. (2003) parameterization is more sensitive to a small change in wind speed than in temperature, and CCN were not strongly affected by changes in wind speed.

It is evident based on this analysis that the changes in wind speed, and therefore local emissions of oceanic aerosols and their precursors, cannot explain all of the simulated marine CCN trends. We will therefore turn to investigating which other factors dampen the effect of natural aerosol emissions on the CCN concentrations.

3.2 The influence of microphysical processes on marine CCN

We estimated the sensitivity of marine CCN concentrations on microphysical processes affecting CCN formation and removal by running a set of high-time-resolution simulations: a reference simulation with all processes included and five simulations where individual processes were turned off. The processes investigated were:

- Primary sea spray
- DMS emissions
- New particle formation
- Nucleation scavenging (rainout)

– Impaction scavenging (washout).

The model was set to provide output every six hours in the selected regions, and run for two months (January–February 1990) using the same spin-up and initial model state as the fifteen-year simulations.

The left-hand panels of Fig. 4 show the simulated CCN concentration in the reference simulation (blue line) and the five sensitivity simulations in the three regions being investigated. It is evident that in all regions, nucleation scavenging (wet removal of aerosol which have been activated as cloud droplets) controls the baseline level of CCN. Without nucleation scavenging (black line), CCN concentrations increase to 2.4 times (Northern Equatorial Pacific), 4.5 times (Southern Ocean), or more than eight times their reference simulation values (North Atlantic). In contrast, simulations without impaction scavenging (wet removal of aerosol particles through collisions with falling raindrops, green line) experience a maximum increase of 20 % in the Northern Equatorial Pacific, where absolute CCN concentrations are higher, and an almost negligible change in the North Atlantic and Southern Ocean.

The inclusion of nucleation scavenging also dampens the extent to which other processes can affect absolute CCN concenentrations. This damping can be seen in the much greater absolute variation between peaks and valleys in the black lines in Figure 4 compared to any of the other simulations. In the North Atlantic, the effect is so extreme that, even after equilibrium has been reached (during the second month), the difference between the maximum and minimum values in the simulation without nucleation scavenging (354.9–196.0 = 158.9 cm^{-3}) is larger than the greatest absolute CCN concentration in any of the other simulations (no impaction scavenging, 105.5 cm^{-3}).

The relative roles of the different processes can be seen more clearly in the right-hand panels of Fig. 4, which show the ratio of CCN in four of the five sensitivity scenarios to CCN in the reference simulation. In the right-hand panels of Fig. 4, the simulation without nucleation scavenging has been omitted to show more detail in the other simulations.

In the Northern Equatorial Pacific (Fig. 4b), CCN are reduced by roughly 10 % of their reference value in simulations without either DMS (orange line) or sea spray (purple line). In the North Atlantic (Fig. 4d), the role of DMS is almost negligible. During the Northern Hemisphere summer, there might be a stronger effect, but our conclusions are unlikely to be affected. On the other hand, switching off sea spray makes a much greater impact on the North Atlantic than on the Northern Equatorial Pacific – about a 30 % decrease on average, with large day-to-day fluctuations.

In both Northern Hemisphere regions, with new particle formation switched off, CCN values fall to about 50 % of their reference simulation values. As we have already seen, DMS contributes a much smaller percentage of CCN in both regions. The majority of precursor vapours participating in new particle formation must therefore have a continental rather than a marine source in these regions.

In the Southern Ocean, natural marine aerosol play a much greater role. Switching off sea spray reduces CCN concentrations by 50 %, and switching off new particle formation decreases CCN by 20–30 % in the summer months. The overlap between simulations without new particle formation and DMS in Fig. 4f shows that the sulphuric acid participating in new particle formation in the Southern Ocean summertime is almost entirely from oceanic sources.

The importance of wind-based processes in the region explains the correlation between Fig. 3e (wind speed) and 3f (CCN). The differences between the wind speed and CCN trends can be attributed to the role of nucleation scavenging, and to the non-local nature of new particle formation in the free troposphere. Woodhouse et al. (2013) showed that DMS emissions must be transported and processed before they affect CCN, meaning that the correlation between sulphate aerosol and local wind speeds will not necessarily be strong. We will also investigate the roles of DMS and continental transport in the following section.

Figure 4 also shows that, when a process is removed, there is a period of adjustment to a new equilibrium value. The length of this adjustment period and the scale of the adjustment vary between processes and regions, providing information on how the system responds. In the case of impaction scavenging and primary sea spray, the adjustment is almost immediate. Without nucleation scavenging, CCN concentrations take approximately three weeks to reach a new equilibrium in all three regions, although there are often large fluctuations about that equilibrium. When new particle formation is switched off, it takes several days for any real response to be seen, but the right-hand panels in Fig. 4 suggest that the simulations have not yet reached their equilibrium values even at the end of the two-month period. New particle formation occurs in the model at heights of more than 15 km, meaning that it takes a long time for the free troposphere to be fully depleted of particles even after the particle formation process has stopped. An equilibrium cannot be reached while particles are still being transported down. The response time to a change in DMS varies according to the local season. In the Southern Ocean, it occurs on approximately the same time scale as the new particle formation response. In the Northern Hemisphere, the response is smaller and slower.

3.3 The influence of continental aerosol on marine CCN

An interesting feature in Fig. 4 is that, most of the time, all six simulations show the same shape of CCN curve, albeit at different absolute levels. We therefore conclude that some other process, not included in the sensitivity runs, controls the fluctuations in the CCN curves. In the Northern Hemisphere regions, continental emissions are an obvious candidate. Since marine organic emissions have not been implemented in GLOMAP, carbonaceous species can act as a fingerprint for continental aerosol in marine regions. We have also confirmed that the carbonaceous aerosol in marine regions originate mainly from continental regions, by means of an additional simulation with ship emissions switched off (not shown). The CCN concentration was almost identical in the simulation without ship emissions, when compared with the reference simulation.

Figure 5 shows a time series of CCN from the high-temporal-resolution reference simulation overlaid onto the simulated accumulation-mode mass of the four aerosol components, which have been scaled to within the CCN range. When continental aerosol make a significant contribution to CCN, the fluctuations in CCN and carbonaceous aerosol should occur at the same time. This coincidence occurs at several points in all three regions, as shown in Fig. 5. However, when carbonaceous aerosol mass is low, there is a better correlation between CCN and other aerosol components. It should be noted that sulphate can have either continental or oceanic origins. An excellent example of the correlation between marine CCN and carbonaceous aerosol occurs in the Northern Equatorial Pacific on day 26 of 1990 (Fig. 5a), when both variables reach their highest values over the two-month period. Even in the Southern Ocean, fluctuations still occur at the same times in each of the sensitivity simulations (for example, just after day 30 in Fig. 4e). Figure 5c shows that, even in this pristine marine region where the majority of CCN are natural in origin, day-to-day fluctuations and the highest concentrations of CCN can both still be attributed to transported continental aerosol.

The role of continental emissions in distorting the correlation between wind speed and CCN trends is further supported by looking at the monthly mean CCN concentrations vs. monthly mean accumulation-mode mass of the four aerosol components over the simulated 15 year period. Figures 6–8 show plots of sulphate (panel a), sea spray (panel b), black carbon (panel c), and organic carbon (panel d) for the three regions being investigated. The Pearson correlation coefficients for the data sets are given in Table 1.

Over the Northern Equatorial Pacific, there is a moderate correlation between CCN concentrations and sulphate (0.58), black carbon (0.54), and organic carbon (0.46). Sea spray mass, on the other hand, behaves independently of CCN concentration, with a correlation coefficient of just 0.05. The presence of carbonaceous aerosol in the soluble accumulation mode indicates that a significant proportion of CCN in the region have been transported from the west coast of North and Central America via prevailing north-easterly trade winds. Since carbonaceous aerosol make such a large contribution to CCN in the region, wind-based sea spray and DMS emissions have less of an effect. This finding is consistent with Spracklen and Rap (2013), who found that anthropogenic aerosol suppressed natural feedbacks, although in their study the divide was between natural and anthropogenic aerosol rather than marine and continental.

The North Atlantic shows an even stronger correlation between CCN and sulphate or carbonaceous aerosol, with correlation coefficients of 0.89 for sulphate and black carbon, and 0.83 for organic carbon. The source of this aerosol is likely to be air pollution from the east coast of North America. However, in this region there is also a moderate anti-correlation with accumulation-mode sea-spray mass, with $R = -0.59$. We speculate that this anti-correlation is due to coagulation losses of CCN with coarse-mode sea spray particles. This suggestion is supported by the anti-correlation between CCN in the simulation without sea spray (purple line) and the simulation without new particle formation (red line) in Fig. 4d.

Although transport of continental aerosol has a strong influence on CCN concentrations, local wind speeds within the polluted regions in the Northern Hemisphere do not correlate with carbonaceous aerosol concentrations. In the North Atlantic, there is an anti-correlation between wind speed and carbonaceous aerosol, probably due to coagulation losses with coarse primary sea spray particles.

The Southern Ocean represents a pristine marine environment, with natural aerosol making up the majority of the accumulation-mode mass. The correlation coefficients are very high for sea spray (0.91) and sulphate (0.82). The high SO_4 correlation coefficient shows the importance of DMS in the region, but Korhonen et al. (2008) also show that continental SO_2 can be transported to the region. However, the correlation coefficients for carbonaceous aerosol are only around 0.14, indicating that on monthly timescales, oceanic aerosol sources are more important, even if some of the day-to-day fluctuations can be attributed to continental aerosol.

In the Northern Equatorial Pacific and North Atlantic, continental aerosol may overwhelm the response to wind trend changes. In the more pristine Southern Ocean region, natural wind-based oceanic aerosols seem to play a greater role.

4 Conclusions

We have used the global aerosol model GLOMAP to investigate the aerosol processes that determine marine CCN concentrations, with a special focus on the effects of observed changes in oceanic surface wind speed. We find that (apart from in the pristine Southern Ocean region), wind speed changes have likely had a negligible effect on marine CCN, mainly due to the more dominant effects of wet scavenging and continental pollution. These results imply that in most marine regions, the predicted changes in surface wind speed are likely to have only a small effect on future CCN, and the resulting aerosol indirect effect will therefore constitute only a minor climate feedback mechanism. On the other hand, changes in precipitation patterns and rates as well as in anthropogenic emissions (e.g., due to transfer to cleaner technologies or air quality legislation) may play much more significant roles. Quantifying the effects of these latter two processes will be the topic of a future study.

Our study highlights the dominant role of nucleation scavenging in regulating marine CCN concentrations, and in dampening the influence of both natural and anthropogenic aerosol sources on the cloud-active particle population over the oceans. Quantification of these damping effects is, however, challenging at present, since previous model intercomparisons have shown significant diversity in the simulated aerosol fields due to different model formulations of this complex sub-grid scale process (Textor et al., 2006). Taken together, these results call for stringent evaluation of aerosol nucleation scavenging parameterizations in large scale models both against observational data and cloud-resolving models. Furthermore, since the removal rate of aerosol due to wet deposition de-

pends on the temporal and spatial coincidence of particles and precipitation, improvements in the global model performance in terms of precipitation patterns and intensities are of key importance.

Acknowledgements. This work was supported by the Academy of Finland through an Academy Research Fellowship (250348) and the associated project funding (256208). We thank Victoria Sinclair, Graham Mann, and Anja Schmidt for helpful discussions.

References

Andres, R. J. and Kasgnoc, A. D.: A time-averaged inventory of subaerial volcanic sulfur emissions, J. Geophys. Res., 103, 25251–25261, 1998.

Arnold, S. R., Chipperfield, M. P., and Blitz, M. A.: A three-dimensional model study of the effect of new temperature-dependent quantum yields for acetone photolysis, J. Geophys. Res., 110, D22305, doi:10.1029/2005JD005998, 2005.

Bates, T. S., Kapustin, V. N., Quinn, P. K., Covert, D. S., Coffman, D. J., Mari, C., Durkee, P. A., De Bruyn, W. J., and Saltzman, E. S.: Processes controlling the distribution of aerosol particles in the lower marine boundary layer during the first aerosol characterization experiment (ACE 1), J. Geophys. Res., 103, 16369–16383, 1998.

Bond, T. C., Streets, D. G., Yarber, K. F., Nelson, S. M., Woo, J.-H., and Klimont, Z.: A technology-based global inventory of black and organic carbon emissions from combustion, J. Geophys. Res., 109, D14203, doi:10.1029/2003JD003697, 2004.

Boucher, O., Randall, D., Artaxo, P., Bretherton, C., Feingold, G., Forster, P., Kerminen, V.-M., Kondo, Y., Liao, H., Lohmann, U., Rasch, P., Satheesh, S. K., Sherwood, S., Stevens, B., and Zhang, X. Y.: Clouds and aerosols, in: Climate Change 2013: The Physical Science Basis. Contribution of Working Group I to the Fifth Assessment Report of the Intergovernmental Panel on Climate Change, edited by: Stocker, T. F., Qin, D., Plattner, G.-K., Tignor, M., Allen, S. K., Boschung, J., Nauels, A., Xia, Y., Bex, V., Midgley, P. M., Cambridge University Press, Cambridge, UK and New York, NY, USA, 571–657, 2013.

Bracegirdle, T. J., Shuckburgh, E., Sallee, J.-B., Wang, Z., Meijers, A. J. S., Bruneau, N., Phillips, T., and Wilcox, L. J.: Assessment of surface winds over the Atlantic, Indian, and Pacific Ocean sectors of the Southern Ocean in CMIP5 models: historical bias, forcing response, and state dependence, J. Geophys. Res.-Atmos., 118, 547–562, 2013.

Chandler, R. and Scott, M.: Statistical Methods for Trend Detection and Analysis in the Environmental Sciences, John Wiley & Sons, Hoboken, New Jersey, 2011.

Chatfield, C.: The Analysis of Time Series: an Introduction, 6th edn., CRC Press, Boca Raton, Florida, 2013.

Chipperfield, M. P.: New version of the TOMCAT/SLIMCAT offline chemistry transport model, Q. J. Roy. Meteor. Soc., 132, 1179–1203, 2006.

Clarke, A. D.: Atmospheric nuclei in the pacific midtroposphere: their nature, concentration, and evolution, J. Geophys. Res., 98, 20633–20647, 1993.

Clarke, A. D., Owens, S. R., and Zhou, J.: An ultrafine sea-salt flux from breaking waves: implications for cloud condensation nuclei in the remote marine atmosphere, J. Geophys. Res., 111, D06202, doi:10.1029/2005JD006565, 2006.

Cofala J., Markus A., and Mechler R.: Scenarios of World Anthropogenic Emissions of Air Pollutants and Methane up to 2030, European Environment Agency (EEA), International Institute for Applied Systems Analysis, Laxemburg, Austria, 2005.

Dee, D. P., Uppala, S. M., Simmons, A. J., Berrisford, P., Poli, P., Kobayashi, S., Andrae, U., Balmaseda, M. A., Balsamo, G., Bauer, P., Bechtold, P., Beljaars, A. C. M., van de Berg, L., Bidlot, J., Bormann, N., Delsol, C., Dragani, R., Fuentes, M., Geer, A. J., Haimberger, L., Healy, S. B., Hersbach, H., Hólm, E. V., Isaksen, L., Kållberg, P., Köhler, M., Matricardi, M., McNally, A. P., Monge-Sanz, B. M., Morcrette, J.-J., Park, B.-

K., Peubey, C., de Rosnay, P., Tavolato, C., Thépaut, J.-N., and Vitart, F.: The ERA-Interim reanalysis: configuration and performance of the data assimilation system, Q. J. Roy. Meteor. Soc., 137, 553–597, 2011.

Dentener, F., Kinne, S., Bond, T., Boucher, O., Cofala, J., Generoso, S., Ginoux, P., Gong, S., Hoelzemann, J. J., Ito, A., Marelli, L., Penner, J. E., Putaud, J.-P., Textor, C., Schulz, M., van der Werf, G. R., and Wilson, J.: Emissions of primary aerosol and precursor gases in the years 2000 and 1750 prescribed data-sets for AeroCom, Atmos. Chem. Phys., 6, 4321–4344, doi:http://dx.doi.org/10.5194/acp-6-4321-200610.5194/acp-6-4321-2006, 2006.

Gantt, B. and Meskhidze, N.: The physical and chemical characteristics of marine primary organic aerosol: a review, Atmos. Chem. Phys., 13, 3979–3996, doi:http://dx.doi.org/10.5194/acp-13-3979-201310.5194/acp-13-3979-2013, 2013.

Guenther, A., Hewitt, C. N., Erickson, D., Fall, R., Geron, C., Graedel, T., Harley, P., Klinger, L., Lerdau, M., Mckay, W. A., Pierce, T., Scholes, B., Steinbrecher, R., Tallamraju, R., Taylor, J., and Zimmerman, P.: A global model of natural volatile organic compound emissions, J. Geophys. Res., 100, 8873–8892, 1995.

Halmer, M. M., Schmincke, H. U., and Graf, H. F.: The annual volcanic gas input into the atmosphere, in particular into the stratosphere: a global data set for the past 100 years, J. Volcanol. Geoth. Res., 115, 511–528, 2002.

Hamilton, J. D.: Time Series Analysis, Princeton University Press, Princeton, New Jersey, 1994.

Harvey, A. C.: Forecasting, Structural Time Series Models and the Kalman Filter, Cambridge University Press, Cambridge, UK, 1990.

Kalnay, E., Kanamitsu, M., Kistler, R., Collins, W., Deaven, D., Gandin, L., Iredell, M., Saha, S., White, G., Woollen, J., Zhu, Y., Leetmaa, A., Reynolds, R., Chelliah, M., Ebisuzaki, W., Higgins, W., Janowiak, J., Mo, K. C., Ropelewski, C., Wang, J., Jenne, R., and Joseph, D.: The NCEP/NCAR 40-year reanalysis project, B. Am. Meteorol. Soc., 77, 437–471, 1996.

Kettle, A. J. and Andreae, M. O.: Flux of dimethylsulfide from the oceans: a comparison of updated data sets and flux models, J. Geophys. Res., 105, 26793–26808, 2000.

Korhonen, H., Carslaw, K. S., Spracklen, D. V., Mann, G. W., and Woodhouse, M. T.: Influence of oceanic dimethyl sulfide emissions on cloud condensation nuclei concentrations and seasonality over the remote Southern Hemisphere oceans: a global model study, J. Geophys. Res., 113, D15204, doi:10.1029/2007JD009718, 2008.

Korhonen, H., Carslaw, K. S., Forster, P. M., Mikkonen, S., Gordon, N. D., and Kokkola, H.: Aerosol climate feedback due to decadal increases in Southern Hemisphere wind speeds, Geophys. Res. Lett., 37, L02805, doi:10.1029/2009GL041320, 2010.

Manktelow, P. T., Carslaw, K. S., Mann, G. W., and Spracklen, D. V.: The impact of dust on sulfate aerosol, CN and CCN during an East Asian dust storm, Atmos. Chem. Phys., 10, 365–382, doi:http://dx.doi.org/10.5194/acp-10-365-201010.5194/acp-10-365-2010, 2010.

Mann, G. W., Carslaw, K. S., Spracklen, D. V., Ridley, D. A., Manktelow, P. T., Chipperfield, M. P., Pickering, S. J., and Johnson, C. E.: Description and evaluation of GLOMAP-mode: a modal global aerosol microphysics model for the UKCA composition-climate model, Geosci. Model Dev., 3, 519–551, doi:http://dx.doi.org/10.5194/gmd-3-519-201010.5194/gmd-3-519-2010, 2010.

Migon, H. S., Gamerman, D., Lopes, H. F., and Ferreira, M. A. R.: Dynamic models, in: Handbook of Statistics

Volume 25: Bayesian Thinking: Modeling and Computation, edited by: Dey, D. and Rao, C. R., Elsevier, Amsterdam, doi: 10.1016/S0169-7161(05)25019-8, 2005.

Monahan, E. C. and Muircheartaigh, I.: Optimal power-law description of oceanic whitecap coverage dependence on wind speed, J. Phys. Oceanogr., 10, 2094–2099, 1980.

Mårtensson, E. M., Nilsson, E. D., de Leeuw, G., Cohen, L. H., and Hansson, H.-C.: Laboratory simulations and parameterization of the primary marine aerosol production, J. Geophys. Res., 108, 4297, doi:10.1029/2002JD002263, 2003.

Nightingale, P. D., Malin, G., Law, C. S., Watson, A. J., Liss, P. S., Liddicoat, M. I., Boutin, J., and Upstill-Goddard, R. C.: In situ evaluation of air-sea gas exchange parameterizations using novel conservative and volatile tracers, Global Biogeochem. Cy., 14, 373–387, 2000.

O'Dowd, C. D., Facchini, M. C., Cavalli, F., Ceburnis, D., Mircea, M., Decesari, S., Fuzzi, S., Yoon, Y. J., and Putaud, J.-P.: Biogenically driven organic contribution to marine aerosol, Nature, 431, 676–680, 2004.

Ovadnevaite, J., Ceburnis, D., Canagaratna, M., Berresheim, H., Bialek, J., Martucci, G., Worsnop, D. R., and O'Dowd, C.: On the effect of wind speed on submicron sea salt mass concentrations and source fluxes, J. Geophys. Res., 117, D16201, doi:10.1029/2011JD017379, 2012.

Partanen, A.-I., Dunne, E. M., Bergman, T., Laakso, A., Kokkola, H., Ovadnevaite, J., Sogacheva, L., Baisnée, D., Sciare, J., Manders, A., O'Dowd, C., de Leeuw, G., and Korhonen, H.: Global modelling of direct and indirect effects of sea spray aerosol using a source function encapsulating wave state, Atmos. Chem. Phys. Discuss., 14, 4537–4597, doi:http://dx.doi.org/10.5194/acpd-14-4537-201410.5194/acpd-14-4537-2014, 2014.

Petris, G., Petrone, S., and Campagnoli, P.: Dynamic Linear Models with R, Springer, New York, 2009.

Pierce, J. R. and Adams, P. J.: Global evaluation of CCN formation by direct emission of sea salt and growth of ultrafine sea salt, J. Geophys. Res., 111, D06203, doi:10.1029/2005JD006186, 2006.

Pringle, K. J.: Aerosol-Cloud Interactions in a Global Model of Aerosol Microphysics, University of Leeds, Leeds, UK, 2006.

Quaas, J., Boucher, O., and Lohmann, U.: Constraining the total aerosol indirect effect in the LMDZ and ECHAM4 GCMs using MODIS satellite data, Atmos. Chem. Phys., 6, 947–955, doi:http://dx.doi.org/10.5194/acp-6-947-200610.5194/acp-6-947-2006, 2006.

Sciare, J., Favez, O., Sarda-Estève, R., Oikonomou, K., Cachier, H., and Kazan, V.: Long-term observations of carbonaceous aerosols in the austral ocean atmosphere: evidence of a biogenic marine organic source, J. Geophys. Res., 114, D15302, doi:10.1029/2009JD011998, 2009.

Sihto, S.-L., Kulmala, M., Kerminen, V.-M., Dal Maso, M., Petäjä, T., Riipinen, I., Korhonen, H., Arnold, F., Janson, R., Boy, M., Laaksonen, A., and Lehtinen, K. E. J.: Atmospheric sulphuric acid and aerosol formation: implications from atmospheric measurements for nucleation and early growth mechanisms, Atmos. Chem. Phys., 6, 4079–4091, doi:http://dx.doi.org/10.5194/acp-6-4079-200610.5194/acp-6-4079-2006, 2006.

Spracklen, D. V. and Rap, A.: Natural aerosol-climate feedbacks suppressed by anthropogenic aerosol, Geophys. Res. Lett., 40, 1–4, 2013.

Textor, C., Schulz, M., Guibert, S., Kinne, S., Balkanski, Y., Bauer, S., Berntsen, T., Berglen, T., Boucher, O., Chin, M., Dentener, F., Diehl, T., Easter, R., Feichter, H., Fillmore, D., Ghan, S., Ginoux, P., Gong, S.,

Grini, A., Hendricks, J., Horowitz, L., Huang, P., Isaksen, I., Iversen, I., Kloster, S., Koch, D., Kirkevåg, A., Kristjansson, J. E., Krol, M., Lauer, A., Lamarque, J. F., Liu, X., Montanaro, V., Myhre, G., Penner, J., Pitari, G., Reddy, S., Seland, Ø., Stier, P., Takemura, T., and Tie, X.: Analysis and quantification of the diversities of aerosol life cycles within AeroCom, Atmos. Chem. Phys., 6, 1777–1813, doi:http://dx.doi.org/10.5194/acp-6-1777-200610.5194/acp-6-1777-2006, 2006.

Tiedtke, M.: A comprehensive mass flux scheme for cumulus parameterization in large-scale models, Mon. Weather Rev., 117, 1779–1800, 1989.

Twomey, S.: Aerosols, clouds and radiation, Atmos. Environ., 25A, 2435–2442, 1991.

Vallina, S. M., Simó, R., and Gassó, S.: What controls CCN seasonality in the southern ocean? A statistical analysis based on satellite-derived chlorophyll and CCN and model-estimated OH radical and rainfall, Global Biogeochem. Cy., 20, GB1014, doi:10.1029/2005GB002597, 2006.

Van Der Werf, G. R., Randerson, J. T., Collatz, G. J., and Giglio, L.: Carbon emissions from fires in tropical and subtropical ecosystems, Glob. Change Biol., 9, 547–562, 2003.

Vautard, R., Cattiaux, J., Yiou, P., Thépaut, J.-N., and Ciais, P.: Northern Hemisphere atmospheric stilling partly attributed to an increase in surface roughness, Nat. Geosci., 3, 756–761, 2010.

Vehkamäki, H., Kulmala, M., Napari, I., Lehtinen, K. E. J., Timmreck, C., Noppel, M., and Laaksonen, A.: An improved parameterization for sulfuric acid-water nucleation rates for tropospheric and stratospheric conditions, J. Geophys. Res., 107, 4622, doi:10.1029/2002JD002184, 2002.

Wanninkhof, R.: Relationship between wind speed and gas exchange over the ocean, J. Geophys. Res., 97, 7373–7382, 1992.

Woodhouse, M. T., Mann, G. W., Carslaw, K. S., and Boucher, O.: Sensitivity of cloud condensation nuclei to regional changes in dimethyl-sulphide emissions, Atmos. Chem. Phys., 13, 2723–2733, doi:http://dx.doi.org/10.5194/acp-13-2723-201310.5194/acp-13-2723-2013, 2013.

Young, I. R., Zieger, S., and Babanin, A. V.: Global trends in wind speed and wave height, Science, 332, 451–455, 2011.

Zheng, X., Albrecht, B., Jonsson, H. H., Khelif, D., Feingold, G., Minnis, P., Ayers, K., Chuang, P., Donaher, S., Rossiter, D., Ghate, V., Ruiz-Plancarte, J., and Sun-Mack, S.: Observations of the boundary layer, cloud, and aerosol variability in the southeast Pacific near-coastal marine stratocumulus during VOCALS-REx, Atmos. Chem. Phys., 11, 9943–9959, doi:http://dx.doi.org/10.5194/acp-11-9943-201110.5194/acp-11-9943-2011, 2011.

Table 1. Pearson coefficients for monthly mean CCN and monthly mean aerosol component mass from the fifteen-year simulations.

Region	Sulphate	Sea Spray	Black Carbon	Organic Carbon
Northern Equatorial Pacific	0.58	0.05	0.54	0.46
North Atlantic	0.89	−0.59	0.89	0.83
Southern Ocean	0.82	0.91	0.13	0.15

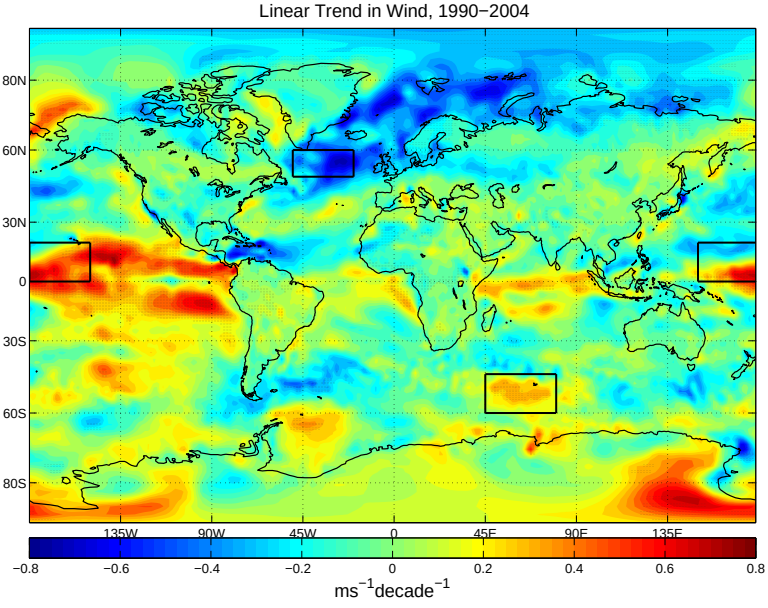

Fig. 1. Linear trend in ERA-Interim ten-metre wind speeds for the years 1990–2004. Stippling shows the areas where the linear trend is statistically significantly different from zero.

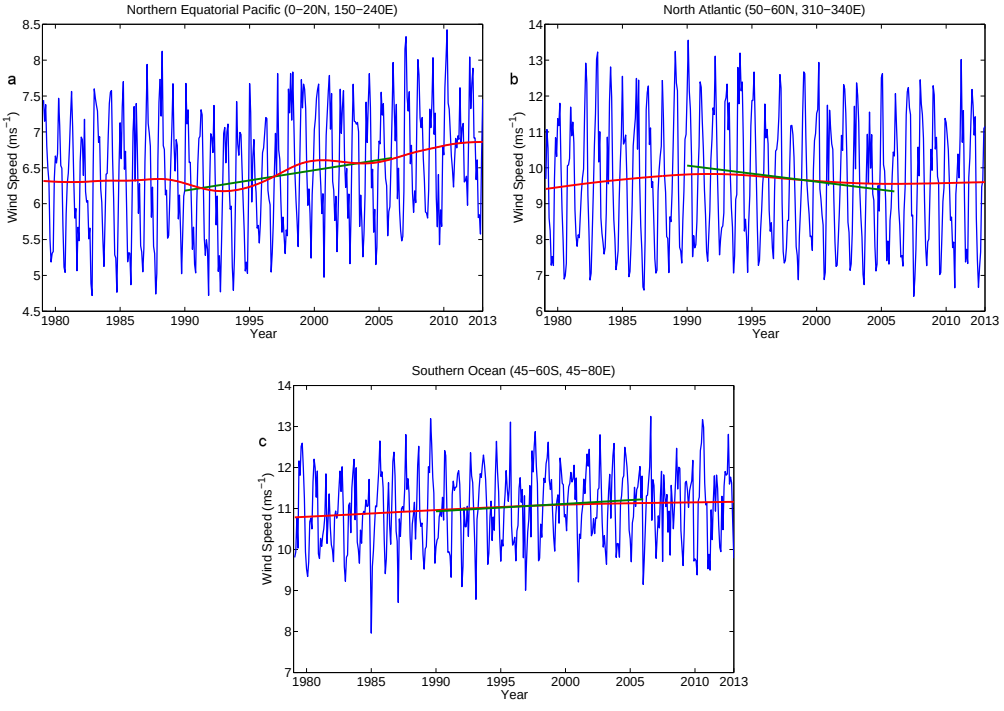

Fig. 2. Comparison of monthly mean values (blue line), linear trend (1990–2004, green line), and locally linear mean level (1979–2012, red line) of ERA-Interim ten-metre wind speed in **(a)** the Northern Equatorial Pacific, **(b)** the North Atlantic, and **(c)** the Southern Ocean. These regions are marked with black boxes in Fig. 1.

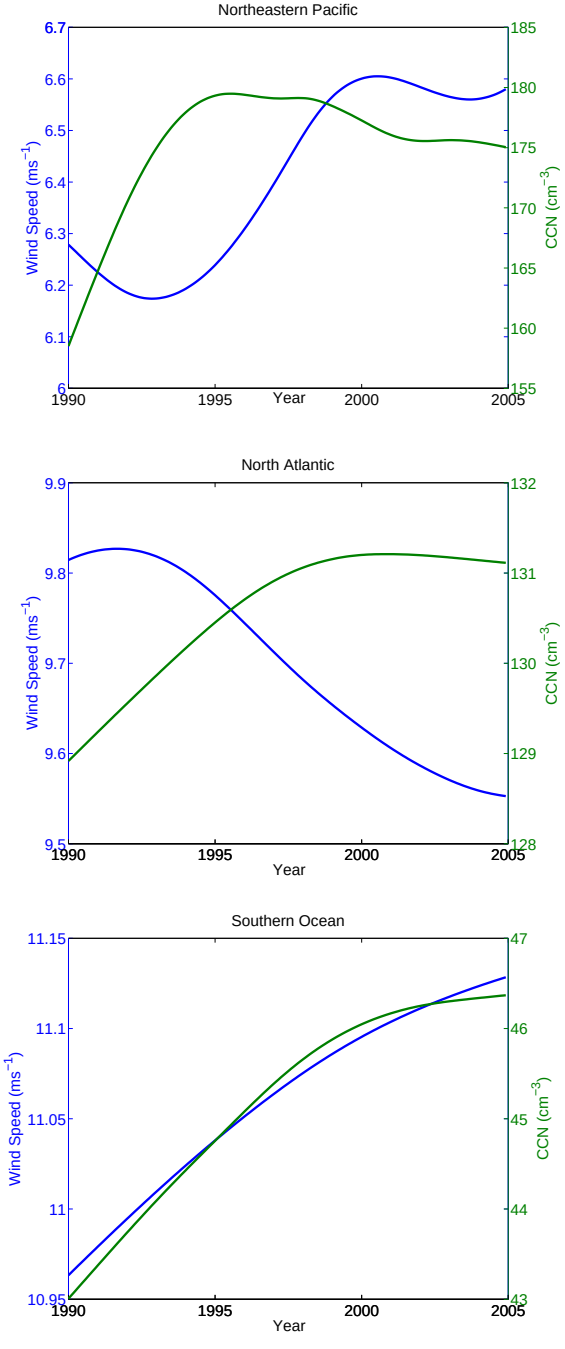

Fig. 3. Trends in wind speed **(a, c, e)** and CCN concentrations **(b, d, f)** in the Northern Equatorial Pacific **(a, b)**, the North Atlantic **(c, d)**, and the Southern Ocean **(e, f)**.

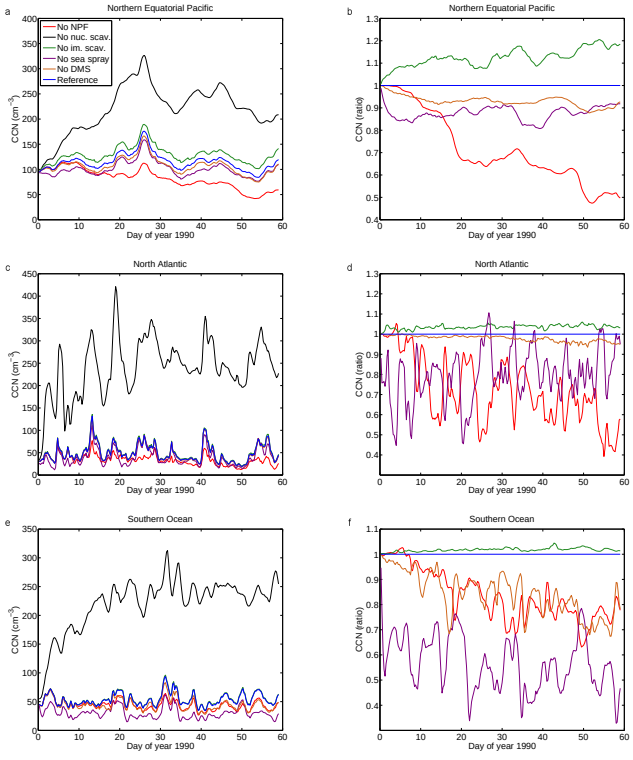

Fig. 4. CCN concentrations (left plots) and ratio to reference concentrations (right plots) at 915 hPa in the Northern Equatorial Pacific **(a, b)**, the Southern Ocean **(c, d)**, and the North Atlantic **(e, f)** in January 1990.

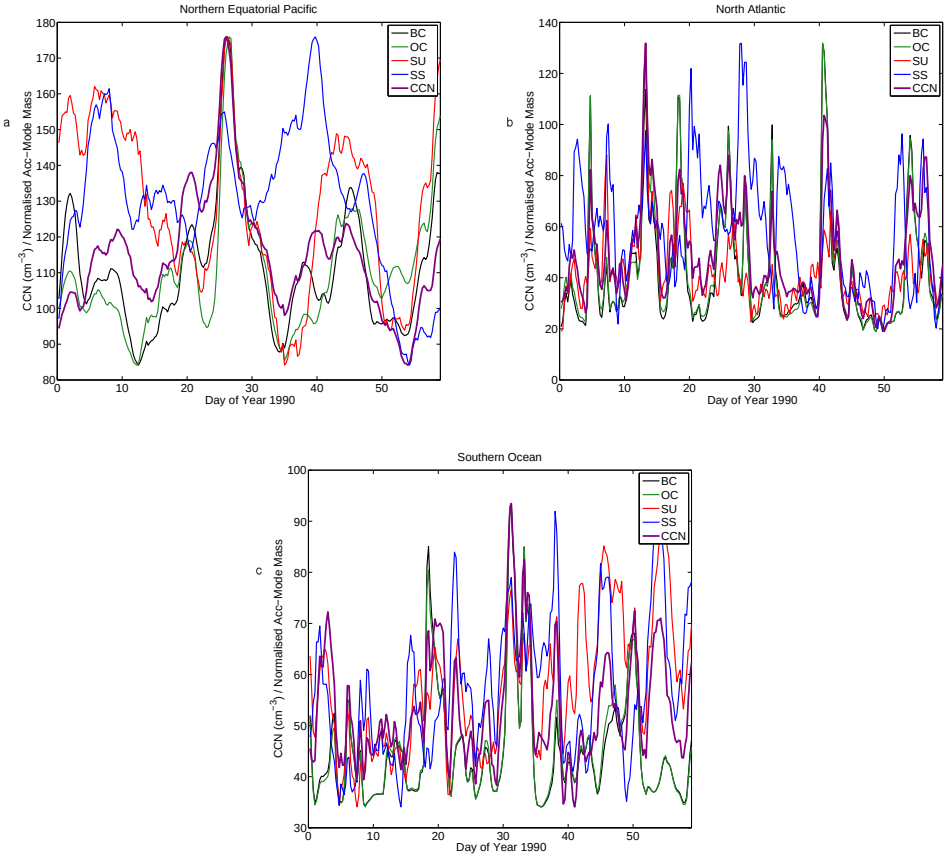

Fig. 5. A time series of scaled accumulation-mode mass of black carbon (black line), organic carbon (green line), sea spray (blue line), and sulphate (red line), overlaid with time series of CCN concentrations (purple line) in the three regions being examined.

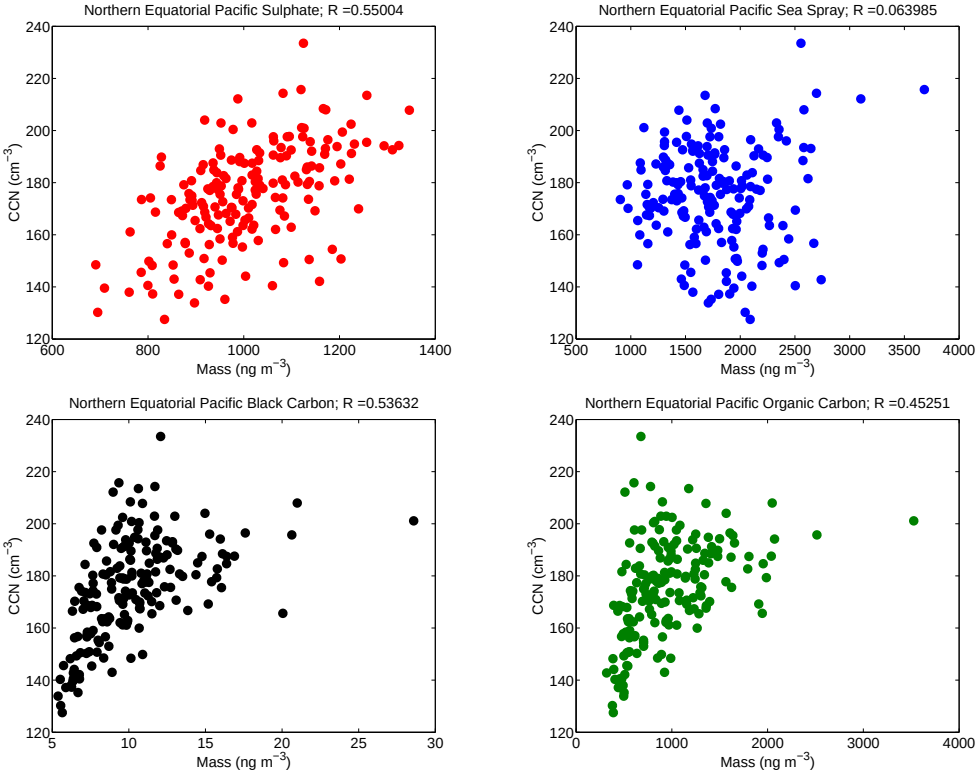

Fig. 6. Scatterplot of simulated monthly mean CCN concentration vs. accumulation-mode mass of **(a)** sulphate, **(b)** sea spray, **(c)** black carbon, and **(d)** organic carbon, in the Northern Equatorial Pacific.

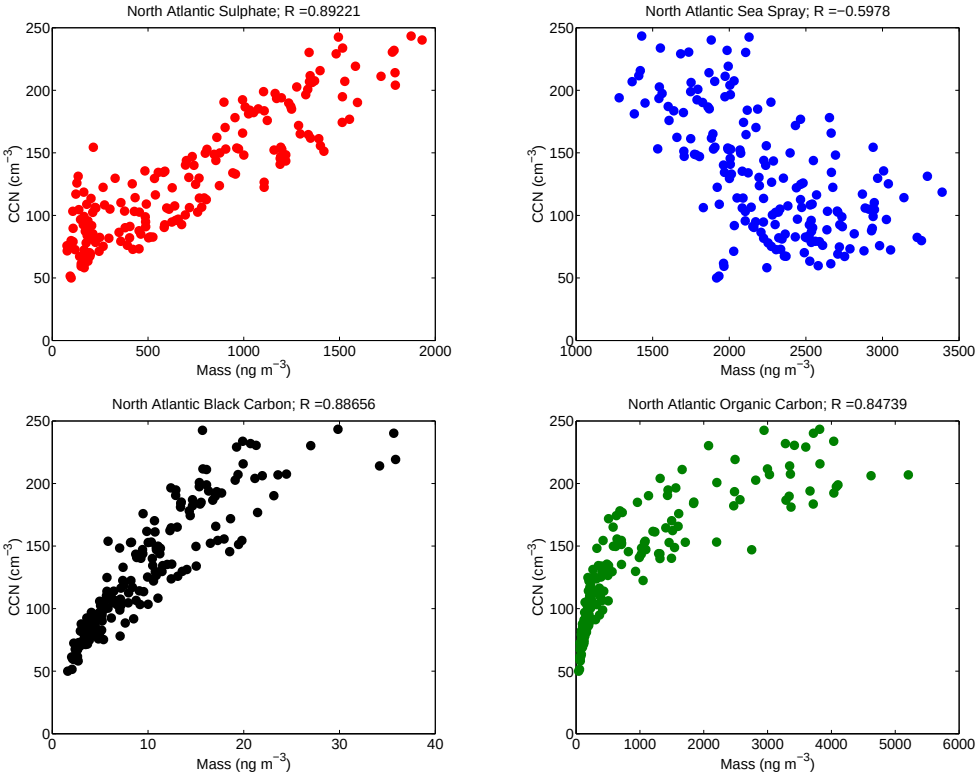

Fig. 7. As for Fig. 6, but for the North Atlantic.

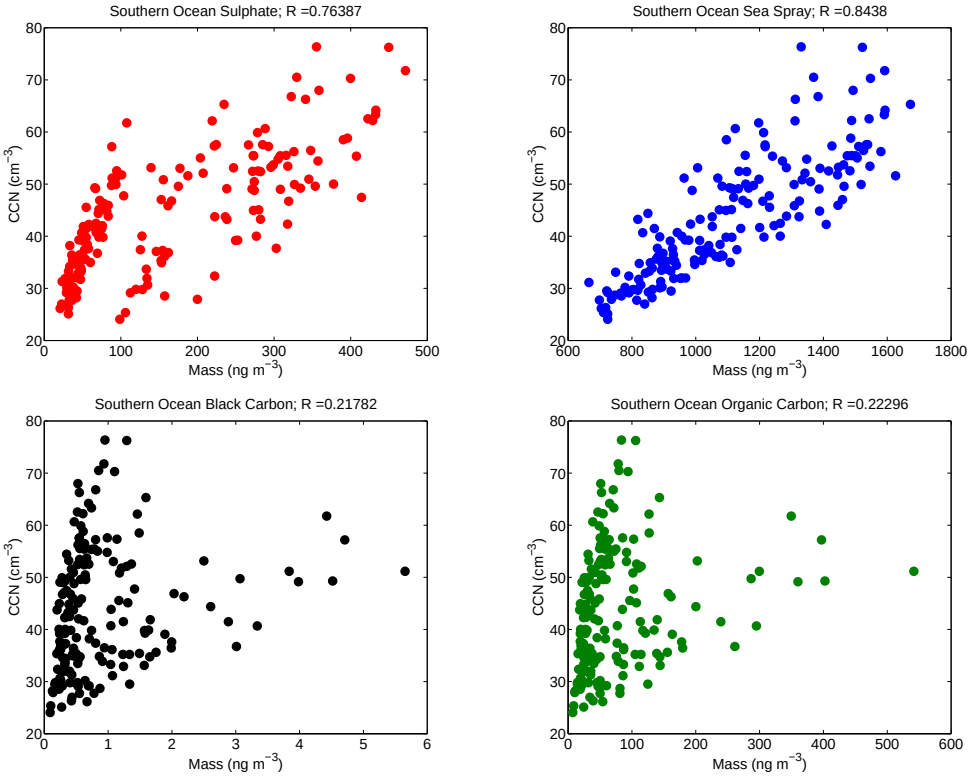

Fig. 8. As for Fig. 6, but for the Southern Ocean.